# **Experimental Procedures**

## **Drosophila Stocks**

 $Pvr^{c02195}$  is a null allele of the Drosophila PDGF/VEGF receptor[1].  $Pvr^{c02859}$  and  $Pvr^{c03211}$  are hypomorphic alleles.  $Vegf17E^{1624ex3}$ , which we term  $Pvf1^{null}$  is a null allele[1] of one of the three Drosophila PDGF/VEGF-like ligands, Pvf1.  $Pvf2^{c06947}$  and  $Pvf3^{EY09531}$  are hypomorphic alleles of Pvf2 and Pvf3 (Bloomington), respectively, while  $Pvf2^{d02444}$  is a UAS-containing EP allele of Pvf2 [1] that allows overexpression of this ligand in the presence of a Gal4 driver. Nrg- $GFP^{G00305}$  contains a protein trap in neuroglian and was used to label epidermal septate junctions[2].

The GAL4/UAS system[3] was used for protein misexpression. A58-Gal4 [4] expresses Gal4 in the larval epidermis, e22c-Gal4 expresses Gal4 in the embryonic and larval epidermis[5], OK376-Gal4 (Bloomington) in the larval fat body and oenocytes, and  $hml\Delta$ -Gal4 in the larval blood cells[6]. A temperature-sensitive Gal4 inhibitor under the control of a ubiquitous promoter[7], tub- $gal80^{ts10A}$ , was combined with UAS- $hep^{ACT(CA)}$  and UAS- $\lambda Pvr$  for temporal control of pathway activation in all larval epidermal cells (A58-Gal4).

UAS-nlacZ (Bloomington) expressed via A58-Gal4 or Pxn-Gal4 [8] was used to label wound sites in X-Gal (5-bromo-4-chloro-3-indolyl-D-galactopyranoside) stained samples for TEM (below) while UAS-Actin-GFP was used to label the epidermal actin cytoskeleton[9] via A58-Gal4. UAS-GFP (Bloomington) was used for comparing tissue specificity of the Gal4 drivers used in this study. The JNK pathway inhibitor, UAS-basket<sup>DN</sup> [10] was used as a positive control for wound closure defects when

overexpressed in the larval epidermis. *UAS-Pvr* and *UAS-Pvf3* [11] were used for overexpression of Pvr and Pvf3, respectively. *UAS-hep*<sup>ACT(CA)</sup> and *UAS-λPvr* were used to constitutively activate the JNK[12] and Pvr[13] signaling pathways, respectively. *w;;msn-lacZ, A58-Gal4/TM6B* and *w;;puc-lacZ, A58-Gal4/TM6B* [4] were used to test for JNK pathway induction upon co-expression of *UAS-DN* or *UAS-RNAi* lines.

(http://www.shigen.nig.ac.jp/fly/nigfly/index.jsp) and the Vienna Drosophila RNAi center were used: 5680R-1 and 5680R-2, targeting basket; 7103 (6173) targeting Pvf1; 13780R-1, 13780R-2, and 13780 (7628) targeting Pvf2; 13781R-1 targeting Pvf3; and 8222R-3 targeting Pvr. UAS-EgfR<sup>DN [14]</sup>, UAS-htl<sup>DN [15]</sup>, UAS-Btl<sup>DN [16]</sup>, and UAS-Btl<sup>RNAi</sup> (Gift of M. Krasnow) were used to inhibit function of the corresponding genes.

The following *UAS-RNAi* lines from NIG-Fly

### **Wounding Assays**

Pinch and puncture wounds were done as described [4]. Briefly, early third instar (L3) *Drosophila* larvae were pinched with blunted forceps or punctured with a 0.1 mm steel needle on the dorsal aspect of a single abdominal segment, usually A4, 5, or 6. Larvae were maintained at 25 °C with the exception of wounding and imaging, which were performed at room temperature. For quantitation of wound closure, wounded larvae were allowed to recover on fly food for 24 hours, a time at which control ( $w^{1118}$ ) wounds were invariably closed. For ease of scoring wound closure we used a live reporter line (Y. Wu and M. Galko, unpublished data) consisting of the *A58-Gal4* driver recombined with a membrane-localized green fluorescent protein and a nuclearly-localized red fluorescent protein. Wounds were scored as "open" if a gap free of nuclei remained in the epidermal

sheet. For visualization, images of dissected and immunostained epidermal wholemounts were captured using a color digital camera (Leica DFC300 FX) and Image-Pro AMS v5.1 Software (Media Cybernetics).

## Wholemount Immunofluorescence and Immunohistochemistry

Dissection and immunostaining of larval epidermal whole-mounts were done as described [4]. Primary antibodies were anti-Fasciclin III [17] (Developmental Studies Hybridoma Bank [DSHB], 1:50); anti-PVR [18] (Jocelyn McDonald, 1:2000); anti-DE-Cadherin[19] (DSHB, 1:20), anti-dp-ERK (Sigma, 1:100), and anti-GFP (Invitrogen, 1:100). Secondary antibodies (Jackson ImmunoResearch or Invitrogen) were goat-anti-mouse Cy3 (1:1000); goat-anti-rabbit-FITC (1:200); goat-anti-rabbit-Cy5 (1:300); and goat-anti-rabbit-Alexa488 (1:). A stock solution of 5 mg/ml 4',6-diamidino-2-phenylindole (DAPI) was used at 1:2,000 to label nuclei and the lipophilic dye FM 1-43FX (5 μg/ml dissolved in Phosphate-buffered saline) was added for 10 minutes at room temperature to unfixed dissected samples to live-label epidermal cell membranes. β-Galactosidase histochemistry to measure JNK activity in *msn-lacZ*- and *puc-lacZ*-expressing larvae was carried out as described in [4] except that the incubations were at 37 °C and the incubation period for *msn-lacZ* was 1.5 hr.

# **Electron Microscopy**

For TEM, larvae were prepared as described[20]. 90 nm sections were observed in a JEOL JEM 1010 transmission electron microscope. Digital photos were obtained using an AMT (Advanced Microscopy Techniques Corp.) imaging system.

## **Actin Cytoskeletal Analysis**

w;;A58-Gal4/TM6B larvae were crossed to w; UAS-actin-GFP (control), w; UAS-actin-GFP, UAS-pvr<sup>RNAi</sup>/Cyo, Act::GFP (experimental), or w; UAS-actin-GFP; UAS-bsk<sup>RNAi</sup>/TM6B (experimental) and progeny larvae were dissected and stained 8 hours post-wounding with anti-GFP. 19 control and experimental larvae viewed under a fluorescent stereomicroscope (Leica MZ16FA) were digitally photographed (Leica DFC300 FX) and given to 3 researchers with no prior knowledge of the experiment. These researchers were asked to bin the blinded photographs into two groups based on undefined morphological criteria. Each researcher correctly binned the larvae into control and experimental groups with 75-80% accuracy, a result that was statistically significant by the Z test for difference in two proportions. For the micrographs in Figure S4, z-stacks of select samples were collected on a Zeiss LSM510 confocal microscope/digital acquisition system.

#### References

- 1. Cho, N.K., Keyes, L., Johnson, E., Heller, J., Ryner, L., Karim, F., and Krasnow, M.A. (2002). Developmental control of blood cell migration by the Drosophila VEGF pathway. Cell *108*, 865-876.
- 2. Morin, X., Daneman, R., Zavortink, M., and Chia, W. (2001). A protein trap strategy to detect GFP-tagged proteins expressed from their endogenous loci in Drosophila. Proc Natl Acad Sci U S A *98*, 15050-15055.
- 3. Brand, A.H., and Perrimon, N. (1993). Targeted gene expression as a means of altering cell fates and generating dominant phenotypes. Development *118*, 401-415.

- 4. Galko, M.J., and Krasnow, M.A. (2004). Cellular and genetic analysis of wound healing in Drosophila larvae. PLoS Biol *2*, E239.
- 5. Lawrence, P.A., Bodmer, R., and Vincent, J.P. (1995). Segmental patterning of heart precursors in Drosophila. Development *121*, 4303-4308.
- 6. Sinenko, S.A., and Mathey-Prevot, B. (2004). Increased expression of Drosophila tetraspanin, Tsp68C, suppresses the abnormal proliferation of ytr-deficient and Ras/Raf-activated hemocytes. Oncogene *23*, 9120-9128.
- 7. McGuire, S.E., Mao, Z., and Davis, R.L. (2004). Spatiotemporal gene expression targeting with the TARGET and gene-switch systems in Drosophila. Sci STKE 2004, pl6.
- 8. Stramer, B., Wood, W., Galko, M.J., Redd, M.J., Jacinto, A., Parkhurst, S.M., and Martin, P. (2005). Live imaging of wound inflammation in Drosophila embryos reveals key roles for small GTPases during in vivo cell migration. J Cell Biol *168*, 567-573.
- 9. Verkhusha, V.V., Tsukita, S., and Oda, H. (1999). Actin dynamics in lamellipodia of migrating border cells in the Drosophila ovary revealed by a GFP-actin fusion protein. FEBS Lett *445*, 395-401.
- 10. Adachi-Yamada, T., Nakamura, M., Irie, K., Tomoyasu, Y., Sano, Y., Mori, E., Goto, S., Ueno, N., Nishida, Y., and Matsumoto, K. (1999). p38 mitogenactivated protein kinase can be involved in transforming growth factor beta superfamily signal transduction in Drosophila wing morphogenesis. Mol Cell Biol 19, 2322-2329.
- 11. Rosin, D., Schejter, E., Volk, T., and Shilo, B.Z. (2004). Apical accumulation of the Drosophila PDGF/VEGF receptor ligands provides a mechanism for triggering localized actin polymerization. Development *131*, 1939-1948.
- 12. Adachi-Yamada, T., Fujimura-Kamada, K., Nishida, Y., and Matsumoto, K. (1999). Distortion of proximodistal information causes JNK-dependent apoptosis in Drosophila wing. Nature *400*, 166-169.
- 13. Duchek, P., Somogyi, K., Jekely, G., Beccari, S., and Rorth, P. (2001). Guidance of cell migration by the Drosophila PDGF/VEGF receptor. Cell *107*, 17-26.

- 14. Perkins, L.A., Johnson, M.R., Melnick, M.B., and Perrimon, N. (1996). The nonreceptor protein tyrosine phosphatase corkscrew functions in multiple receptor tyrosine kinase pathways in Drosophila. Dev Biol *180*, 63-81.
- 15. Beiman, M., Shilo, B.Z., and Volk, T. (1996). Heartless, a Drosophila FGF receptor homolog, is essential for cell migration and establishment of several mesodermal lineages. Genes Dev *10*, 2993-3002.
- 16. Reichman-Fried, M., and Shilo, B.Z. (1995). Breathless, a Drosophila FGF receptor homolog, is required for the onset of tracheal cell migration and tracheole formation. Mech Dev *52*, 265-273.
- 17. Patel, N.H., Snow, P.M., and Goodman, C.S. (1987). Characterization and cloning of fasciclin III: a glycoprotein expressed on a subset of neurons and axon pathways in Drosophila. Cell *48*, 975-988.
- 18. McDonald, J.A., Pinheiro, E.M., and Montell, D.J. (2003). PVF1, a PDGF/VEGF homolog, is sufficient to guide border cells and interacts genetically with Taiman. Development *130*, 3469-3478.
- 19. Oda, H., Uemura, T., Harada, Y., Iwai, Y., and Takeichi, M. (1994). A Drosophila homolog of cadherin associated with armadillo and essential for embryonic cell-cell adhesion. Dev Biol *165*, 716-726.
- 20. Babcock, D.T., Brock, A.R., Fish, G.S., Wang, Y., Perrin, L., Krasnow, M.A., and Galko, M.J. (2008). Circulating blood cells function as a surveillance system for damaged tissue in Drosophila larvae. Proc Natl Acad Sci U S A *105*, 10017-10022.

### **Supplemental Discussion**

The model described here is reminiscent of the initiation of coagulation in vertebrates, where exposure of blood-borne Factor VII to Tissue factor on extravascular cell surfaces activates the formation of a fibrin clot[1]. Thus, although the specific molecular players may be distinct, it appears that exposure of blood-derived signals to extravascular tissue is a critical damage-sensing mechanism in both flies and vertebrates, despite the vastly different architectures of their barrier tissues and circulatory systems.

In addition to revealing a novel mode of sensing the wound, our work identifies a potential cellular role of JNK signaling in epidermal wound closure—mediating the transient dedifferentiation of wound-edge epidermal cells. Unlike in mice, JNK does not appear to be upstream of production of an EGF-like ligand[2], since interfering with EGFR signaling did not affect wound closure in our assay. The distinct loss and gain of function phenotypes of JNK and Pvr suggests that JNK activation is not a downstream consequence of Pvr activation, as it appears to be in *Drosophila* thorax closure[3]. This finding is important because it implies that there is a distinct wound-induced signal that activates JNK and allows wound-edge epidermal cells to shut off cuticle synthesis and adhesion. A general role for the JNK pathway in dedifferentiation was suggested by a recent study of transdifferentiation in *Drosophila* imaginal discs[4], where JNK was found to be required for suppression of Polycomb group proteins that serve to maintain cellular fates. It will be interesting to determine if similar nuclear reprogramming is transiently required during larval wound healing.

Finally, our work raises the interesting possibility that there might be a conserved autocrine role for VEGF/VEGFR signaling in epidermal wound closure. VEGF-A, the closest vertebrate homolog of Pvf1[5], is, like Pvf1, constitutively expressed by epidermal keratinocytes[6]. A keratinocyte-specific conditional knockout of VEGF-A led to a slight delay of wound closure at 12-15 days post-wounding[7] and an increased distance between the epidermis and the underlying dermal vasculature. Although the defect in wound closure was interpreted as a consequence of the defect in wound neovascularization, the recent finding that VEGFRs are expressed on primary human keratinocytes and can mediate chemotactic migration of these cells *in vitro*[8-10], raises the intriguing possibility that epidermally secreted VEGFs have autocrine as well as paracrine functions during vertebrate wound closure. The experimental test of this hypothesis, analyzing wound closure in mice with a conditional deletion of VEGFRs in keratinocytes, has not yet been reported.

#### References

- 1. Krupiczojc, M.A., Scotton, C.J., and Chambers, R.C. (2008). Coagulation signalling following tissue injury: Focus on the role of factor Xa. Int J Biochem Cell Biol *40*, 1228-1237.
- 2. Li, G., Gustafson-Brown, C., Hanks, S.K., Nason, K., Arbeit, J.M., Pogliano, K., Wisdom, R.M., and Johnson, R.S. (2003). c-Jun Is Essential for Organization of the Epidermal Leading Edge. Developmental Cell *4*, 865-877.
- 3. Ishimaru, S., Ueda, R., Hinohara, Y., Ohtani, M., and Hanafusa, H. (2004). PVR plays a critical role via JNK activation in thorax closure during Drosophila metamorphosis. Embo J *23*, 3984-3994.

- 4. Lee, N., Maurange, C., Ringrose, L., and Paro, R. (2005). Suppression of Polycomb group proteins by JNK signalling induces transdetermination in Drosophila imaginal discs. Nature *438*, 234-237.
- 5. Andrae, J., Gallini, R., and Betsholtz, C. (2008). Role of platelet-derived growth factors in physiology and medicine. Genes Dev *22*, 1276-1312.
- 6. Brown, L.F., Yeo, K.T., Berse, B., Yeo, T.K., Senger, D.R., Dvorak, H.F., and van de Water, L. (1992). Expression of vascular permeability factor (vascular endothelial growth factor) by epidermal keratinocytes during wound healing. J Exp Med *176*, 1375-1379.
- 7. Rossiter, H., Barresi, C., Pammer, J., Rendl, M., Haigh, J., Wagner, E.F., and Tschachler, E. (2004). Loss of vascular endothelial growth factor a activity in murine epidermal keratinocytes delays wound healing and inhibits tumor formation. Cancer Res *64*, 3508-3516.
- 8. Brem, H., Kodra, A., Golinko, M.S., Entero, H., Stojadinovic, O., Wang, V.M., Sheahan, C.M., Weinberg, A.D., Woo, S.L., Ehrlich, H.P., et al. (2009). Mechanism of Sustained Release of Vascular Endothelial Growth Factor in Accelerating Experimental Diabetic Healing. J Invest Dermatol.
- 9. Man, X.Y., Yang, X.H., Cai, S.Q., Yao, Y.G., and Zheng, M. (2006). Immunolocalization and expression of vascular endothelial growth factor receptors (VEGFRs) and neuropilins (NRPs) on keratinocytes in human epidermis. Mol Med *12*, 127-136.
- 10. Wilgus, T.A., Matthies, A.M., Radek, K.A., Dovi, J.V., Burns, A.L., Shankar, R., and DiPietro, L.A. (2005). Novel function for vascular endothelial growth factor receptor-1 on epidermal keratinocytes. Am J Pathol *167*, 1257-1266.

# **Supplementary Figure legends**

Figure S1. Specificity of Gal4 Drivers Used in this Study

Dissected wholemounts of third instar larvae expressing UAS-GFP via A58-Gal4 (A,E,I,M), e22c-Gal4 (B,F,J,N), Fat body-Gal4 (C,G,K,O), and  $hml\Delta$ -Gal4 (D,H,L,P). (A,B) A58-Gal4 and e22c-Gal4 drive GFP expression in the epidermis. A58-Gal4 appears to be the stronger driver since fluorescence intensity is greater even though e22c-Gal4 commences expression in the embryo. (C,D) Fat body-Gal4 and hml∆-Gal4 do not drive expression in the epidermis, except in scattered cells at a very low level (white triangle) for  $hml\Delta$ -Gal4. (E) A58-Gal4 does drive GFP expression in the fat body. (F) e22c-Gal4 does not drive GFP expression in the fat body. (G,H) Fat body-Gal4 also drives expression in the larval fat body while hml∆-Gal4 does not. (I, J, K) A58-Gal4, e22c-Gal4, and Fat body-Gal4 do not drive expression in the blood cells which are visualized in the epidermal wound gap 4 hr post pinch wounding. (L) hmlΔ-Gal4 does drive expression in wound adherent blood cells as well as circulating blood cells (not shown). (M,N,O,P) Higher magnification DIC images of blood cells in boxed areas in (I,J,K,L). Other sites of expression observed in live or dissected wholemounts (not shown) are as follows: e22c-Gal4- hindgut, tracheal dorsal trunks, scattered fat body cells, and low levels in brain; Fat body-Gal4- salivary gland, subset of cells in proventriculus, tracheal dorsal trunks;  $hml\Delta$ -Gal4- subset of cells in proventriculus, lymph gland hemocytes; A58-Gal4- tracheal dorsal trunks, subset of cells in proventriculus, salivary glands, and malpighian tubules. Importantly, the only drivers which fail to rescue the Pvf1<sup>null</sup> mutant when expressing UAS-Pvf1 express strongly in the

epidermis. Conversely, those which do rescue express in the fat body or blood cells but not the epidermis. Scale bars =  $100\mu m$ .

Figure S2. Pvr is Localized to the Lateral Epidermal Cell Membrane and its Expression is Upregulated After Wounding

(A) Confocal z-stacks of a dissected and immunostained larva of the genotype *w*, *Nrg-GFP* shown in X-Y plane (top) and X-Z projection (bottom) along the membrane indicated with a white line. Nrg-GFP (green) localizes to epidermal membranes along most of the apico-basal axis. DE-cadherin (red) localizes to the apical aspect of epidermal membranes. Pvr (blue) localizes to epidermal membranes along most of the apico-basal axis. Merge, all channels shown. Asterisk, apical (cuticle) side; arrowhead, basal side. (B) Dissected epidermal wholemounts of unwounded (left panel) or pinch wounded (middle and right panels) *w*<sup>1118</sup> and *UAS-bsk*<sup>RNAi</sup>-expressing (via *A58-Gal4*) larvae immunostained with anti-Pvr. Epidermal Pvr protein levels increase 4 hours after wounding. Scale bars in (A), 50 μm (top panels); 10 μm (bottom panels).

Figure S3. ERK is Activated Independently of Pvr Signaling After Wounding Dissected epidermal wholemounts of an unwounded segment (top panel) and puncture-wounded segments (middle and bottom panels) of a third instar  $w^{1118}$  larva and a larva expressing  $UAS-Pvr^{RNAi}$  via A58-Gal4 larvae (bottom panel) immunostained with anti-dp-ERK. Wounded segments exhibit intense staining (red) in cells immediately proximal to the wound site.

Figure S4. Knockdown of Pvr and JNK signaling have different effects on the woundedge actin cytoskeleton (A-D) Dissected epidermal wholemounts of wounded L3 larvae containing *A58-Gal4* crossed to *UAS-actin-GFP* (A), *UAS-actin-GFP*; *UAS-bsk*<sup>RNAi</sup> (B), or *UAS-actin-GFP*, *UAS-Pvr*<sup>RNAi</sup> (C, D). At eight hours post-wounding control larvae exhibit profuse actin-based extensions of varying widths and lengths into the dark (top) wound gap (A) while *UAS-bsk*<sup>RNAi</sup> expressing larvae exhibit normal projections but a brighter concentration of actin at the wound edge (B). By contrast, *UAS-Pvr*<sup>RNAi</sup> expressing larvae exhibit mostly smooth wound borders (D) with sparse, mostly wide, projections (C). Bar in (A), 20 μm for (A-D).

Figure S5. JNK Activation is Independent of Pvr Signaling During Wound Healing (A-H) Dissected wholemounts of pinch wounded third instar larvae stained with X-Gal to detect β-Galactosidase activity six hours post wounding. (A-D) *w;;msn-lacZ, A58-Gal4* larvae expressing no UAS (A), *UAS-bsk*<sup>DN</sup> (B), *UAS-bsk*<sup>RNAi</sup> (C), or *UAS-Pvr*<sup>RNAi</sup> (D). (E-H) *w;;puc-lacZ, A58-Gal4* larvae expressing no UAS (E), *UAS-bsk*<sup>DN</sup> (F), *UAS-bsk*<sup>DN</sup> (G), or *UAS-Pvr*<sup>RNAi</sup> (H). (A), or expressing, *w, UAS-bsk*<sup>DN</sup> (B,F), *w;;UAS-bsk*<sup>RNAi</sup> (C,G), or *w;UAS-Pvr*<sup>RNAi</sup> (D,H). (A,E) Control larvae induce *msn-lacZ* and *puc-lacZ* JNK reporter expression in epidermal cells surrounding the wound. (B,F) *UAS-bsk*<sup>DN</sup>-expressing larvae show greatly reduced reporter expression surrounding wounds. (C, G) *UAS-bsk*<sup>RNAi</sup>-expressing larvae show reduced reporter expression surrounding wounds. (D, H) *UAS-Pvr*<sup>RNAi</sup>-expressing larvae induce JNK reporter expression around the wound border at levels comparable to controls (compare to (A) and (E).

Figure S6. Ectopic Epidermal Activation of JNK and Pvr Leads to Distinct Cellular Phenotypes

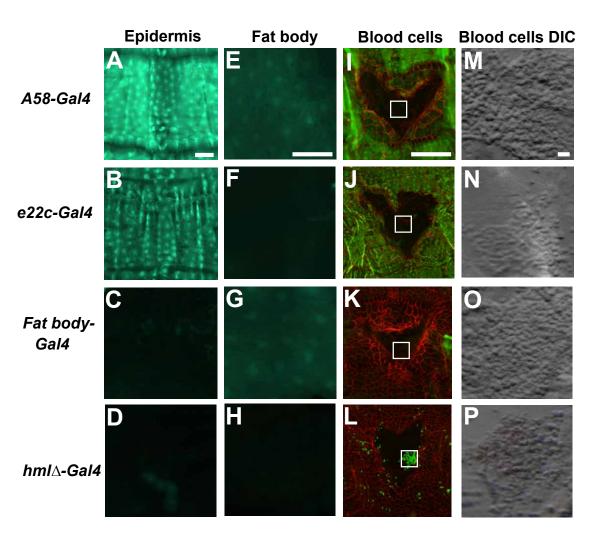
(A-L) Dissected wholemounts of third instar w;tub-gal80<sup>ts10</sup>/+;A58-Gal4 larvae expressing no UAS (control; A, D, G, J), UAS-hep<sup>Act</sup> (B, E, H, K) or UAS-λPvr (C, F, I, L). (A-F) Fasciclin III immunostaining labels epidermal cell membranes (red). (A) Control epidermis, low magnification of single larval body segment. Temperature shift does not affect uniformity in size and shape of epidermal cells. (B) Constitutive activation of JNK 16 hours after temperature shift results in loss of Fasciclin 3 staining. (C) Constitutive activation of Pvr 16 hours after temperature shift results in irregular epidermal cell shapes. (D) Close up of (A). (E) Close up of (B). (F) Close up of (C). (G-I) DAPI staining. (G) DAPI staining of (D)- control epidermal cells are mononuclear. (H) DAPI staining of (E) shows presence of nuclei despite loss of Fasciclin III staining indicating cells are still adherent to the cuticle. (I) DAPI staining of (F) shows presence of nuclei. (J-L) FM 1-43FX membrane dye labels epidermal membranes (center, green). Dashed white lines indicate borders of larval body wall muscles to sides of epidermal sheet. (J) Epidermal cell membranes are apparent between the body wall muscles. (K) Loss of epidermal cell membranes on expression of UAS $hep^{Act}$ . (L) Membranes are retained on expression of  $UAS-\lambda Pvr$  and may label more intensely than control. Vertical line, same sample. Scale bars, 100 µm.

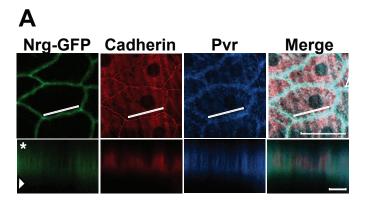
Figure S7. Temperature-dependence of etopic epidermal Pvf1 expression interfering with epidermal wound closure

To test the hypothesis that it is overexpression of Pvf1 that interferes with closure upon ectopic epidermal expression via the A58-Gal4 driver, we tested the temperature-dependence of this interference and plotted % open wounds versus genotype/temperature. Consistent with the idea that the excess ligand becomes available to bind Pvr after wounding and that this interferes with the normal spatial presentation of the ligand, we find that lowering the temperature (and thus the level of ectopic Pvf1) does in fact lead to an attenuation (partial rescue) of the  $PvfI^{null}$  wound closure defect. N = 30 larvae per genotype per temperature.

Figure S8 Blood cell-expressed Pvf1 can rescue the wound closure defect of *Pvf1*<sup>null</sup> mutant larvae

Control larvae ( $w^{1118}$ ; $hml\Delta$ -Gal4/+) showed almost completely closed wounds while  $PvfI^{Null}/Y$ ; $hml\Delta$ -Gal4/+ larvae showed a fully penetrant wound closure defect. Ectopic blood cell expresson of UAS-PvfI in a wild-type background ( $w^{1118}$ ; $hml\Delta$ -Gal4/UAS-PvfI) causes a slight wound closure defect ( $\sim$ 20 %) which may be due to the scattered small patches of low-level epidermal expression observed with this driver (Figure S1) while ectopic blood cell expression of UAS-PvfI in a  $PvfI^{null}$  mutant background ( $PvfI^{Null}/Y$ ; $hml\Delta$ -Gal4/UAS-PvfI) rescues the wound closure defect from 100 % to  $\sim$  22 %. N = 30-34 larvae per genotype.





В

